



AMERICAN METEOROLOGICAL SOCIETY

Journal of Applied Meteorology and Climatology

EARLY ONLINE RELEASE

This is a preliminary PDF of the author-produced manuscript that has been peer-reviewed and accepted for publication. Since it is being posted so soon after acceptance, it has not yet been copyedited, formatted, or processed by AMS Publications. This preliminary version of the manuscript may be downloaded, distributed, and cited, but please be aware that there will be visual differences and possibly some content differences between this version and the final published version.

The DOI for this manuscript is doi: 10.1175/JAMC-D-16-0232.1

The final published version of this manuscript will replace the preliminary version at the above DOI once it is available.

If you would like to cite this EOR in a separate work, please use the following full citation:

Scott, A., B. Zaitchik, D. Waugh, and K. O'Meara, 2016: Intra-urban temperature variability in Baltimore. *J. Appl. Meteor. Climatol.* doi:10.1175/JAMC-D-16-0232.1, in press.

© 2016 American Meteorological Society



Intra-urban temperature variability in Baltimore

Anna A. Scott*

Johns Hopkins University, Baltimore, Maryland.

Ben Zaitchik

Johns Hopkins University, Baltimore, Maryland.

Darryn Waugh

Johns Hopkins University, Baltimore, Maryland.

Katie O'Meara

Architectural Design, Maryland Institute College of Art, Baltimore, Maryland, USA.

*Corresponding author address: Department of Earth and Planetary Sciences, Johns Hopkins University, Baltimore, Maryland, USA.

E-mail: annascott@jhu.edu

ABSTRACT

13 How much does minimum daily air temperature vary within neighborhoods
14 exhibiting high LST and does this variability effect agreement with the near-
15 est weather station? To answer this, a low cost sensor network of 135 iBut-
16 ton thermometers was deployed for summer 2015 in Baltimore City, a mid-
17 sized American city with a temperate climate, focusing on an underserved
18 area exhibiting high land surface temperatures (LST) from satellite imagery.
19 The sensors were evaluated against commercial and NOAA-NWS stations
20 and showed good agreement for daily minimum temperatures. Variability
21 within the study site was small: mean minimum daily temperatures have a
22 spatial standard deviation of 0.9°C , much smaller than the same measure for
23 satellite-derived land surface temperature. The sensor-measured temperatures
24 agree well with the NOAA-NWS weather station in downtown Baltimore,
25 with a mean difference for all measurements in time and space of 0.00°C ;
26 this agreement with the station is not found to be correlated with any mete-
27 orological variables with the exception of radiation. Surface properties are
28 found to be important in determining spatial variability: vegetated or green
29 spaces are observed to be 0.5°C cooler than areas dominated by impervious
30 surfaces and the presence of green space is found to be a more significant pre-
31 dictor of temperature than surface properties such as elevation. Other surface
32 properties—albedo, tree canopy cover and distance to the nearest park—are
33 not found to correlate significantly with air temperatures.

³⁴ **1. Introduction**

³⁵ Extreme temperature is now the deadliest form of climate hazard worldwide (WMO 2014), and
³⁶ heat waves, extended periods of elevated heat and humidity, are a growing problem in most of
³⁷ the United States (IPCC 2013). The health impacts of heat waves are potentially exacerbated by
³⁸ growing urban populations as well as the urban heat island (UHI) effect, a land-atmosphere inter-
³⁹ action causing cities to be several degrees hotter than rural areas. The effect is most pronounced
⁴⁰ at night and thus understood to be caused by urban-rural differences in cooling rates (Oke 1982).

⁴¹ Temperature differences between cities and rural surroundings have been measured around the
⁴² world (Oke 1982). These measurements have typically been taken assuming an idealized city with
⁴³ a densely populated, highly urbanized core surrounded by more vegetated and sparsely populated
⁴⁴ suburbs. Correspondingly, temperature is schematized as decreasing with radial distance from the
⁴⁵ dense urban core.

⁴⁶ Less well quantified is variability within the urban heat island (Arnfield 2003), which in some
⁴⁷ cases has been documented to be as large as the urban-rural difference or enough to offset it
⁴⁸ (Jonsson 2004). A number of recent studies have started closing this gap through installing *in*
⁴⁹ *situ* monitoring networks (for example, Chapman et al. (2015a); Schatz and Kucharik (2014);
⁵⁰ Mikami et al. (2003); Smoliak et al. (2015)) or using private networks (for example, Hardin (2015)
⁵¹ analyses data from NOAA and Earth Networks, Inc.'s UrbaNet). However, these networks are not
⁵² yet widespread (for a recent list of such networks, refer to Schatz and Kucharik (2014)), and
⁵³ their focus on urban-rural differences smooths over neighborhood and sub-neighborhood level
⁵⁴ variability which may be of interest to urban planners. Many cities have an urban weather station
⁵⁵ with data that are available to researchers and decision makers. The term urban describes a wide
⁵⁶ range of characteristics in the built and natural environment, and so urban stations may be located

57 in areas which differ markedly enough in characteristics from residential neighborhoods to affect
58 their temperature readings by up to several degrees (Stewart and Oke 2012). Understanding how
59 temperatures may differ from a centrally monitored temperature is critically important to health
60 professionals and urban planners, who may rely on central stations to assess the health burden of
61 heat, issue local heat-related weather alerts and closures, or target UHI mitigation strategies.

62 One way to assess spatial variability within the urban heat island is through satellite-derived
63 land surface temperature (LST). Some progress has been made developing algorithms to derive
64 air temperature from LST (Ho et al. 2014; Sun et al. 2005; Kloog et al. 2014), but this is not yet
65 widespread and numerous urban heat island studies use LST (e.g., Zhao et al. (2014); Nichol et al.
66 (2009); Xu and Liu (2015); Ho et al. (2016); White-Newsome et al. (2013)). Although LST is not
67 equivalent to the 2-meter air temperature of concern to human comfort, a number studies show a
68 relationship between the surface urban heat island and the urban heat island as measured by air
69 temperature (Voogt and Oke 2003; Arnfield 2003; Nichol and To 2012), and living in an area with
70 high LSTs has been associated with higher mortality during periods of high heat (Smargiassi et al.
71 2009; Laaidi et al. 2012; Harlan et al. 2013; Hondula et al. 2012).

72 We aim to ask, how much does minimum daily air temperature vary within neighborhoods ex-
73 hibiting high LST and does this variability effect agreement with the nearest weather station. We
74 address this question using measurements from Baltimore, Maryland, USA, a mid-sized American
75 city on the Chesapeake Bay. Satellite-derived land surface temperature shows spatial variability
76 within the Baltimore, including the tendency for downtown areas to be warmer than tree-lined
77 areas on the urban periphery (Fig. 1). Satellite measurements show that the hottest neighborhoods
78 are characterized by little vegetation, few trees, and impervious surfaces; they are also the most
79 underserved economically (Huang et al. 2011). In such locations, satellite land surface tempera-
80 tures can exceed those of downtown by 5-10 degrees Celsius. Baltimore experiences hot, humid

81 summers and has a Köppen-Geiger climate classification of Cfa, indicating a warm temperate cli-
82 mate, year-round humidity and precipitation, and hot summers (Peel et al. 2007). Accordingly, the
83 City of Baltimore considers heat stress management to be a top priority for disaster preparedness
84 and climate change adaptation (Baltimore 2013). The boxed area in Fig. 1 is the target of city
85 interventions to reduce energy use and potentially temper the UHI through urban greening ini-
86 tiatives. Specifically planned are planting additional street trees, creating pocket parks, focusing
87 community outreach and education efforts, and installing so-called cool roofs (roofs made with
88 highly reflective paint or other covering) in the target neighborhoods. While a number of studies
89 circumstantially support the use of urban greening to cool an urban area, most use models or satel-
90 lite data to fill in the sporadic station availability common in most urban areas (Bowler et al. 2010).
91 A number of studies from past decades have examined the effects of urbanization on urban heat-
92 ing as cities have grown, notably in Columbia, Maryland (Landsberg 1979), or Phoenix, Arizona
93 (Balling and Brazel 1987), but it is exceedingly rare to have the chance to study urban modifica-
94 tions as they are implemented. Critical to this is a baseline understanding of urban temperature
95 variability at the sub-neighborhood scale before any changes are implemented.

96 This paper presents results from a dense, low-cost air temperature sensor network in Baltimore
97 (Fig. 1) in an unprecedented characterization of air temperature at sub-neighborhood resolution.
98 This network is part of larger interdisciplinary urban heat island project (Zaitchik et al. 2016).
99 Our measurements focus on extensively sampling a thermal hot spot in East Baltimore (see boxed
100 inset of Fig. 1) using a network of iButton thermometer/hygrometers and weather stations from
101 NOAA-NWS and Davis Instruments. We discuss and validate our temperature sensors in Section
102 2. The spatial variability of the network and the connection with surface properties is presented in
103 Section 3, and finally some implications for urban policy are discussed in Section 4.

104 **2. Materials and Methods**

105 *a. Observations*

106 Data used in this paper come from a NOAA-NWS weather station, a Davis Instruments Vantage
107 Pro-2 weather station, satellites, and a network of Maxim Integrated iButtons. The iButtons pro-
108 vide a stand alone thermometer, hygrometer and data logger the size of a standard watch battery
109 and have a reported accuracy of $.5^{\circ}\text{C}$ for the temperature ranges seen during the reporting period.
110 This accuracy was confirmed in laboratory conditions by a random sample of 30 of the buttons
111 (not shown). The iButton and a radiation shield are attached with plastic zip ties to trees (90.4%),
112 wooden posts (2.2%), or metal lampposts or street signs (7.4%) and removed at the end of the
113 summer recording period.

114 The iButtons cost relatively little (approximately 70 US dollars for the iButton) for an out-of-
115 the-box measuring and data-logging solution. Together they provide a low-profile micro-weather
116 station that fits in the palm of a hand and may be installed discreetly in neighborhoods with high
117 foot traffic (Fig. 2). Having a discreet sensor allows us to quickly expand the range of monitoring
118 locations beyond our own neighborhoods and social networks.

119 We began installing the network of iButtons in June 2015 and left them to record hourly tem-
120 perature through mid-September (Fig. 3). More iButtons were added throughout the summer to
121 refine measurements for a total of 153 iButtons. One round of data collection occurred during
122 mid-July. By the time of sensor collection in October, 135 remained. Results were checked for
123 different time periods and found to be insensitive of the period of data analysis: changes in the
124 sensor network did not impact our conclusions. Data collection focused on East Baltimore neigh-
125 borhoods and placed sensors approximately 150 meters apart on five transects, three East/West,
126 and two North/South, ranging from 1.6 to 4 kilometers long. Additional iButtons were installed

127 in neighborhood parks and near weather stations for data validation. Most of the landscapes in
128 this area are homogeneous. Two or three story brick rowhouses are the main housing stock (Fig.
129 2a), corresponding to a local climate zone (LCZ) 3 or compact low-rise (Stewart and Oke 2012).
130 Much of the landscape variability comes from the presence of trees (LCZ B, scattered trees) or
131 grass and vegetation (LCZ D, low plants), as seen in Fig. 2b, although the center of the transects
132 passes through a four block by four block urbanized zone (LCZ 1, or compact high-rise) that is
133 home to the Johns Hopkins Medical campus.

134 Each iButton was installed facing north. At each installation location, scientists recorded the
135 landcover as impervious, grass, or soil, the installation site (trees, metal poles, or wood posts), and
136 estimated the amount of shade as full shade, partial shade, or none (that is, full sun). Landcover
137 takes into account the ambient conditions as opposed to the purely local conditions. For example, a
138 tree sitting in a tree well with exposed soil would be listed as impervious if the surrounding area is
139 concrete or asphalt, and a sensor in a vegetated but vacant lot is specified as being in a green space
140 even if the sensor is not located in a park or in an official city green space. Shade measurements,
141 by comparison, are purely local and only take into account the estimated amount of sunlight that
142 the sensors receive. Figure 2 illustrate typical sites that were both listed as partial shade; 5.9% of
143 sensors were in full sun, 45.2% were in partial shade, and 48.9% were in full shade.

144 As noted in Chapman et al. (2015b) and WMO (2010), urban air temperature sampling comes
145 with unique challenges. Standard meteorological sighting protocols are often inapplicable in urban
146 areas, and it was particularly challenging to find any locations for sensor installation that reflect
147 the average ambient conditions in many of the neighborhoods studied in this paper. For example,
148 trees are thought to be a source of urban cooling (Kleerekoper et al. 2012), but our sampling
149 methodology relies on the presence of at least a few trees. A majority of the iButtons were installed
150 on trees (90.4%), but occasionally, no trees were available in what would be considered average

151 residential conditions, causing sampling to shift to locations in vacant and vegetated lots or wooded
152 alleyways. This is perhaps one form of sampling bias. Additionally, brick rowhouses dominate the
153 landscape (see Fig. 2) and release heat at night, which may cause street-adjacent readings to differ
154 from those taken farther from buildings. In spite of these challenges, we argue that our sampling
155 method reasonably balances the need for rigorous meteorological standards with the need for data
156 in an under-studied environment.

157 In addition to the iButton network, daily temperature data is also available from a NOAA-NWS
158 weather station located in downtown Baltimore at the Maryland Science Center, hereafter referred
159 to as the downtown station (Fig. 3). We used a 15-year record to calculate an extreme tem-
160 perature threshold from the 95th percentile of minimum daily temperature. As the downtown
161 station is only 15 years old, we checked this threshold against a longer period (1975-2014) at
162 the Baltimore-Washington International Airport NOAA-NWS synoptic station, approximately 12
163 kilometers SSW of the study site. The two extreme temperature thresholds were found to be con-
164 sistent with their mean difference of 2°C. NOAA-NWS station thermometers are aspirated and
165 have a reported accuracy of .56°C (Diamond et al. 2013).

166 Hourly meteorological data (wind, pressure, relative humidity, and radiation) are also taken from
167 a Davis Instruments Vantage Pro-2 weather station installed at Johns Hopkins University on the
168 roof of Olin Hall (referred to as the JHU Station). A similar station was installed mid-summer in
169 East Baltimore at two meter height in the greened interior of a residential block; the JHU station
170 wind and radiation data was checked against this data and not found to differ significantly. For
171 continuity's sake, only the JHU station data was used. The Vantage Pro-2 has a reported accuracy
172 of .5°C for the temperature ranges seen during the reporting period and is naturally aspirated.

173 A number of satellite-derived observations are also used. Landsat 8 (LP DAAC 2015) from
174 10:46 AM local time on July 16, 2016, the least cloudy image available for the observation period,

175 was used to calculate both LST and albedo. Nighttime Landsat scenes are not available for this
176 period. To derive LST, band 10 digital number (DN) data is converted to the top of atmosphere
177 at-sensor radiance and then at-satellite brightness temperature following (Jiménez-Muñoz and So-
178 brino 2003). To account for the different surface emissivities, we use the USGS land cover map
179 to categorize the brightness temperatures by land type, and assign them an emissivity value as
180 in Alipour et al. (2003). Subsequently, we apply a correction for atmospheric water vapor to the
181 brightness temperature following the mono-window algorithm in Qin et al. (2001). Climatolog-
182 ical temperature from the weather station at Johns Hopkins is used to determine the surface air
183 temperature, which is then used to estimate atmospheric temperature aloft.

184 The Landsat 8 scene was also used to calculate albedo using a normalized form of Liang (2001)
185 as outlined in Smith (2010). Satellite-derived tree canopy data at 10-foot resolution (Fig. 3) was
186 provided by TreeBaltimore. Elevation data comes from the Maryland Lidar dataset for Baltimore
187 City (USGS 2015) and the park shapefile data was downloaded from Baltimore OpenData.

188 *b. Measurement Evaluation*

189 iButtons come pre-calibrated for laboratory settings, but meteorological air temperature must be
190 measured in the shade (WMO 2010). Shielding is then the principal source of error for outdoor
191 temperature measurements, though poor aspiration or sighting thermometers near sources of heat
192 can also contribute to error. The iButtons and shield used in this study were evaluated against
193 a Vantage Pro-2 naturally aspirated weather station and an aspirated NOAA-NWS station. The
194 results, shown in Figure 4, indicate that sensors agree well with station data for minimum daily
195 temperatures. Diurnal results indicate that while sensors agree at night, significant differences are
196 detected during daytime hours (2°C or more). As the daytime differences between the iButton
197 and station temperatures were not well correlated with humidity, wind speed, or incoming solar

radiation, they are omitted from this analysis. While micro-climate differences may be exaggerated during the day, we argue that a focus on daily minimum temperatures makes sense in the context of the urban heat island, a phenomena that is maximized at night and largely disappears during the daytime. The greatest need for local data is then at night and in the early morning; thus, temperatures are collected hourly for the period of June 1 to September 15 2015 and sub-sampled to obtain $T = T_{min}(x_i, t)$, a time-series of daily minimum temperatures at each sample location x_i . This dataset (Scott et al. 2016) is available for download through the Johns Hopkins Data Archive at <https://archive.data.jhu.edu/dvn/>. Minimum daily temperatures occur at approximately 6 am, at which time the mean wind speed is $0.37 m.s^{-1}$ and mode of the wind direction is North-Northeast, although minimum temperatures may not occur simultaneously at each location.

3. Results

The spatial variability of minimum daily air temperatures measured in East Baltimore is smaller than expected. For the summertime (temporal) mean of daily minimum temperatures seen in Fig. 3, the standard deviation is $0.9^{\circ}C$, which is small compared to the seasonal range of $20^{\circ}C$ and small even in the context of the range of temporal mean temperatures, $4.15^{\circ}C$. The distribution of all observed air temperatures is nearly normal (Fig. 5a), with a temporal-spatial mean temperature $\langle \bar{T} \rangle = 21.7^{\circ}C$. Here, $\langle T \rangle$ refers to spatially averaged temperature, and \bar{T} refers to temporally averaged temperature. This value was calculated by averaging first over time at each sensor and then over space.

The distribution of temperature (Fig. 5a) measured at the downtown station is similar to the distribution of temperatures in East Baltimore. The mean and range of East Baltimore and the downtown station are also similar, and when East Baltimore and station data are plotted as a time series (Fig. 5b) very little difference is discernible. The summer of 2015 experienced several periods of

extreme heat, seen where the station temperature exceeds the extreme heat threshold, as well as cooler periods (Fig. 5b); this day-to-day meteorological variability contributes to the wide range of temperatures seen in the histograms and explains why the reported standard deviation of temporal mean temperatures, 0.9°C , is much smaller than the standard deviation of all data, 2.78°C . The distribution of temperature differences with the downtown station, $\Delta T(x_i, t) = T_i - T_{downtown}$, is nearly normal (Fig. 5c), and has a low standard deviation ($\sigma = 1.37$); these statistics were computed by equally weighting each measurement in space and time. The mean difference $\overline{\Delta T(x_i, t)} \approx 0.00^{\circ}\text{C}$ is negligible, and much less than the precision of either the iButton or downtown station thermometer. As nearly all of the data falls within $\pm 2^{\circ}\text{C}$, then we conclude that the downtown Baltimore station is a reasonable way to assess average thermal conditions in East Baltimore.

Mean agreement with the weather station does not appear to vary with weather conditions. This was assessed by correlating meteorological variables with the spatial mean temperature difference with the downtown station $\langle \Delta T \rangle(t) = \langle T_i - T_{downtown} \rangle$ (Fig. 6a,c,e,g). Meteorological variables are calculated as the mean of the previous day (i.e., lagged one day), and the correlation coefficient r is calculated as the Pearson product-moment correlation coefficient. The observation period covered several periods of extreme heat (Fig. 5 b), however, the correlation between the previous day's temperature and spatially averaged daily $\langle \Delta T \rangle$ is insignificant ($r = 0.003$, two-tailed p-value $p = .98$, Fig. 6a), indicating periods of extreme heat do not affect agreement with the downtown station. Increased wind speed, pressure, and radiation all had insignificant correlations with temperature difference (Fig. 6c,e,g). The insignificance of these correlation values lead us to conclude that mean sensor agreement is not explained by meteorological conditions.

Additionally, much of the variability in observed air temperature in Fig. 5 is due to temporal variability rather than spatial variability. First, the downtown station and the sensor network have the same standard deviation ($\sigma = 2.8$, Fig. 5a). When the data is time-averaged and this

245 meteorological variability is removed, the standard deviation falls from 2.78°C to 0.9°C . Sec-
246 ond, sensor-to-sensor agreement with the downtown station does not correlate significantly with
247 meteorological variables except for radiation (Fig. 6b,d,f,h). This was assessed by correlating
248 meteorological variables with $\sigma(\Delta T) = \sigma(T(x_i) - T_{downtown})$, the time-varying spatial standard
249 deviation of agreement with the station. This measure assesses the sensor-to-sensor variability
250 in station agreement or more broadly, temperature variability in the spatial sense. There are in-
251 significant correlations ($|r| < 0.1$, $p > .2$) with mean temperature, wind speed, and pressure. The
252 correlation of radiation with temperature variability (Fig. 6h, $r = 0.25$, $p < 0.05$) is the only sig-
253 nificant correlation, and shows that sunnier conditions increase the chance that a given sensor may
254 disagree with the downtown station. We note, however, that the variability is still small, around a
255 degree or so.

256 The spatial variability of East Baltimore air temperature is also much less than what is suggested
257 by daytime LST in Fig. 1. Satellite-derived urban-rural differences are largest during the day,
258 whereas the air temperature differences are largest at night, so even though minimum daily T_{air} and
259 daytime satellite temperature measurements do not occur at the same time, they are comparable in
260 the sense that both may be used to assess the UHI intensity. As expected, the mean of minimum
261 daily air temperatures is much lower than that of LST: $\langle \bar{T} \rangle = 21.1^{\circ}\text{C}$ as compared to $\langle LST \rangle =$
262 43.3°C , respectively. The standard deviation σ and range R of air temperature are also lower
263 than those of LST: $\sigma(\bar{T}) = 0.9^{\circ}\text{C}$ as compared to $\sigma(LST) = 2.07^{\circ}\text{C}$, and $R(\bar{T}) = 4.15^{\circ}\text{C}$ versus
264 $R(LST) = 7.9^{\circ}\text{C}$. The discrepancy between air temperature and LST in the mean, variability and
265 range shows the potential caveats of using LST and air temperature interchangeably to diagnose
266 the severity of urban heating.

267 Much of the sensor-to-sensor spatial variability can then be explained by variability in land
268 cover, and in particular whether a sensor is placed in an area dominated by impervious or green

space. Green spaces, or spaces dominated by grass and other vegetation, are cooler than impervious spaces on average by 0.56°C (Fig. 5a). While small, the difference is found to be significant by a Welch's t-test (p-value of 1.9×10^{-10} using the Python library Scipy's `stats.ttest_ind` function (Jones et al. 2001)). This difference explains 12% of the variability in mean minimum daily temperature. Green spaces are also on average cooler than the downtown station, whereas impervious spaces are slightly warmer, though this difference is slight: $\langle \Delta T \rangle_{green} = -0.18^{\circ}\text{C}$ versus $\langle \Delta T \rangle_{imp.} = +0.39^{\circ}\text{C}$. As meteorological standards encourage sighting weather stations around fields and vegetated areas (WMO 2014), it is important to note that micro-climate effects may influence temperature when using standard weather station data to assess local urban conditions even at night.

Nighttime temperatures correlate insignificantly with other surface properties (Fig. 7), with the exception of elevation. The relationship between surface properties and temperature was assessed by correlating elevation, albedo, a sensor's distance from an official park, and the calculated percent tree canopy cover for a 33 square meter box centered around the sensor with time-averaged \bar{T} . For green spaces, only elevation correlates significantly with \bar{T} . Tree canopy, elevation, and albedo correlate insignificantly. None of the examined surface variables correlate significantly with temperatures taken in impervious spaces. The insignificant correlations with park distance may be affected by using the official inventory of park locations—the City of Baltimore runs an adopt-a-lot program that allows citizens and community groups to manage vacant lots as parks, gardens, or green spaces without formal recognition, so many of the sensors which were counted in green space were not in official parks, especially in neighborhoods where there are fewer parks. This suggests that the larger parks did not have an impact on temperature outside of their boundaries. Air temperature is also not correlated significantly with LST (Fig. 8), with $p > .75$ for both green and impervious spaces. While LST is not a surface property as it changes over time,

293 it is highly correlated with static surface properties such as distance to park ($r = 0.6$). LST and
294 air temperature are both used as measures to diagnose urban heating, so it is notable that on the
295 neighborhood scale the correlation is so poor.

296 Regression analysis confirms that the presence of green space is a predictor of mean air temper-
297 ature, and the only reliable predictor of the aspects examined (LST, albedo, distance to park, and
298 tree canopy cover). Ordinary least squares regression with elevation and presence of green space
299 (1 for green space, 0 for impervious) against mean daily minimum temperature gives the following
300 result :

$$\bar{T} = 21.3 - 0.01x_{elevation} - 0.51x_{greenspace}$$

301 which explains 11% of the variability ($r^2 = 0.11$). Elevation is included because it correlated
302 strongly with green space temperature ($r = -0.36$) and because green space occurs at a range of
303 elevations (0-60 m). Only presence of green space is statistically significant at the 95% confidence
304 level ($p = 0.000$ for green space, $p = 0.11$ for elevation). Other tested variables were co-linear, for
305 example, albedo and tree cover, and so could not produce a robust regression result. The regres-
306 sion coefficient for $x_{greenspace}$ indicates that after controlling for elevation, temperatures decrease
307 by 0.5°C when entering a green space. This is more than the mean difference of $.6^\circ\text{C}$ between im-
308 pervious and green space indicated in Fig. 5a; as green space is more abundant at lower elevations
309 (Fig. 7a), this suggests that elevation is masking some of the cooling effects of parks and green
310 spaces.

311 4. Discussion

312 Though previous studies have shown that parks are around a degree cooler during the day
313 (Bowler et al. 2010), it was unexpected that green spaces would be cooler at night. While dur-
314 ing the day, latent heat release in parks and vegetated areas is probably the source of cooling, at

night, condensation could cause warming. To explain this, we can offer some hypotheses, although an analysis of the mechanisms for urban cooling are beyond the scope of this paper. Taking the approach of Oke et al. (1991), the net energy budget of the urban surface can be understood to be: $L + S + R = Q_{net}$ where L represents latent heat flux, S represents sensible heat flux, R the radiative heat flux, and Q_{net} the residual flux, which is non-zero throughout the course of the day. As wind speed during the nighttime hours is low, sensible heat is low, enhanced radiative cooling could explain why that parks are efficient at nighttime cooling. This is further influenced by differing material properties, such as the thermal capacity, conductance, and emissivity. Geometry, and in particular the sky view factor, may also play a role as parks tend to be more open and thus have greater radiative loss. While we do not presently see a relationship between park size and temperature, this is limited by the study area and number of parks present in this study, and so we cannot generalize. Perhaps a larger scale study could find such a connection.

Our conclusions that wind speed, as measured at weather stations, appears to be less important than surface properties is interesting in light of a recent UHI study in Birmingham, UK, where wind speed and direction was found to play an important role in governing urban heating (Azevedo et al. 2016). While a number of studies in the literature have found that low wind speeds would allow for more temperature heterogeneity within the urban heat island (e.g., Oke (1982); Schatz and Kucharik (2014)), our study found insignificant relationships between daily wind speed and temperature differences with the station. This suggests that any changes associated with increasing wind speed are experienced uniformly within the study area.

As our climate warms, more cities seek cost-effective strategies to cool their neighborhoods, such as greening plans that increase the amount of vegetated surfaces and increase tree canopy (e.g., Kleerekoper et al. (2012)). While this paper is not intended to evaluate these strategies, our findings suggest some possible limitations to interventions implemented at the neighborhood scale,

especially for the levels of vegetation found in East Baltimore. Our analysis does find that vegetated spaces are significantly cooler than impervious spaces, but this effect is found to be small and very localized: only 0.5°C even after controlling for the effects of elevation. This is not sufficient to offset urban heating, which is often several degrees or more. One possible policy intervention supported by this work is local greening near where residents are likely to congregate, such as planting more and smaller parks or grass sidewalk right-of-ways in residential areas. Presently, our results would support greening policies that begin with planting grass or other low vegetation rather than tree planting. We caution that the low tree cover canopy amounts present in our study area (most locations had tree canopy coverage of 0-30%) may prevent drawing conclusions about the potential of increasing tree canopy, as the overall tree canopy in this neighborhood is low. While these ranges of tree canopy were not found to be sufficient to cool impervious surfaces, there may still be a threshold level above which this isn't true.

We also caution that differing climate zones and city landscapes may prevent the results of this study from being directly applied to other areas. One lesson we think will apply to other cities is how geo-spatial relationships with surface properties may change according to scale; findings that apply at the city-wide scale may not be relevant at the neighborhood and sub-neighborhood level. This has the possibility to complicate possible policy interventions. We found this to be true for relationships between air temperature and LST: we found that the point-to-point correlation between LST and air temperature was poorer than what was indicated in the literature. Such studies looked at this relationship on larger scales, however (e.g., Kloog et al. (2014); Nichol and To (2012); Nichol et al. (2009)). This conclusion agrees with White-Newsome et al. (2013), who found a poor correlation between LST and air temperature when comparing point to point, but had better results when average LST at radii of larger than 200m. This may also be true for other variables, such as tree canopy cover, or albedo.

363 **5. Conclusion**

364 Summertime air temperature measurements in Baltimore, Md. using 135 low-cost air temper-
365 ature sensors show that much of the spatial variability in daily minimum air temperature is small
366 and that some of this variability (11%) is explained by surface properties, namely, the presence or
367 absence of vegetation, and not well explained by meteorology. The time-averaged minimum daily
368 temperatures have a spatial standard deviation (0.9) that is much smaller than the same measure
369 for satellite-derived land surface temperature (2.07), and the sensor-measured temperatures agree
370 well with the NOAA-NWS weather station in downtown Baltimore, with an mean difference for
371 all measurements in time and space of 0.00°C . The presence or absence of vegetation affected
372 temperature more than other meteorological and surface properties examined, and time-averaged
373 air temperatures in green spaces are found to be cooler than impervious spaces by about 0.5°C .

374 This work suggests that using thermal satellite imagery to estimate the variability of minimum
375 daily air temperatures will exaggerate air temperature variability and care must be used when us-
376 ing thermal imagery in place of *in situ* air temperature measurements in order to diagnose urban
377 heating. As the mean differences with the downtown weather station are not statistically signifi-
378 cant, these findings support the use of the downtown weather station in Baltimore to assess average
379 thermal conditions even in thermally-identified hot spots.

380 This work raises a number of questions. As discussed above, an open question is why green
381 spaces are cooler at night. Another question is whether our findings will hold when examined on a
382 city-wide basis. More work is ongoing to determine this. Hopefully this will help answer questions
383 about how densely temperature must be monitored to capture the sub-neighborhood variability of
384 interest to our partners in public health and urban planning. This study examined areas that were
385 largely homogeneous in terms of the built environment, but for a geographically expanded study,

³⁸⁶ pairing data with a standard measure of urbanization or classification such as a brightness index
³⁸⁷ or the local climate zone classification could help comparisons with ongoing work in other cities.

³⁸⁸ *Acknowledgments.* We acknowledge Kristin Baja and the Baltimore City Department of Sus-
³⁸⁹ tainability, NSF IGERT grant DGE-1069213, NSF Hazards SEES grant # 1331399, and the Johns
³⁹⁰ Hopkins Department of Earth and Planetary Science summer field fund for their support, as well
³⁹¹ as Clara Hickman, Sophie Stoerkel and the Maryland Institute College of Art for the radiation
³⁹² shield design. We also thank Erik Jorgensen, Jasmin Gonzalez, Dillon Ponzo, and Celine Sze
³⁹³ for their invaluable help with fieldwork, as well as Emma Eklund for her work on satellite data.
³⁹⁴ Our community partners helped greatly with community outreach and helped guide our installa-
³⁹⁵ tion process; in particular, we thank Beth Meyers-Edwards and Banner Neighborhoods as well as
³⁹⁶ Jennifer Kunze and the Amazing Grace Evangelical Lutheran Church.

³⁹⁷ References

- ³⁹⁸ Alipour, T., M. Sarajian, and A. Esmaeily, 2003: Land surface temperature estimation from ther-
³⁹⁹ mal band of landsat sensor, case study: Alashtar city. *The International Achieves of the Photo-*
⁴⁰⁰ *togrammetry, Remote Sensing and Spatial Information Sciences*, **38**, 4.
- ⁴⁰¹ Arnfield, A. J., 2003: Two decades of urban climate research: a review of turbulence, exchanges
⁴⁰² of energy and water, and the urban heat island. *International Journal of Climatology*, **23** (1),
⁴⁰³ 1–26, doi:10.1002/joc.859, URL <http://dx.doi.org/10.1002/joc.859>.
- ⁴⁰⁴ Azevedo, J. A., L. Chapman, and C. L. Muller, 2016: Quantifying the daytime and night-time
⁴⁰⁵ urban heat island in birmingham, uk: A comparison of satellite derived land surface temperature
⁴⁰⁶ and high resolution air temperature observations. *Remote Sensing*, **8** (2), 153.

- 407 Balling, R. C., and S. W. Brazel, 1987: Time and space characteristics of the Phoenix urban heat
408 island. *Journal of the Arizona-Nevada Academy of Science*, **21** (2), 75–81, URL <http://www.jstor.org/stable/40024889>.
- 410 Baltimore, C. o., 2013: City of baltimore disaster preparedness and planning project (dp3). *City of*
411 *Baltimore Office of Sustainability, Baltimore, MD.*
- 412 Bowler, D. E., L. Buyung-Ali, T. M. Knight, and A. S. Pullin, 2010: Urban greening to cool towns
413 and cities: A systematic review of the empirical evidence. *Landscape and Urban Planning*,
414 **97** (3), 147 – 155, doi:<http://dx.doi.org/10.1016/j.landurbplan.2010.05.006>, URL <http://www.sciencedirect.com/science/article/pii/S0169204610001234>.
- 416 Chapman, L., C. L. Muller, D. T. Young, E. L. Warren, C. S. B. Grimmond, X.-M. Cai, and E. J. S.
417 Ferranti, 2015a: The Birmingham Urban Climate Laboratory: An open meteorological test bed
418 and challenges of the smart city. *Bulletin of the American Meteorological Society*, **96** (9), 1545–
419 1560, doi:[10.1175/BAMS-D-13-00193.1](https://doi.org/10.1175/BAMS-D-13-00193.1), URL <http://dx.doi.org/10.1175/BAMS-D-13-00193.1>,
420 <http://dx.doi.org/10.1175/BAMS-D-13-00193.1>.
- 421 Chapman, L., C. L. Muller, D. T. Young, E. L. Warren, C. S. B. Grimmond, X.-M. Cai, and E. J. S.
422 Ferranti, 2015b: The birmingham urban climate laboratory: An open meteorological test bed
423 and challenges of the smart city. *Bulletin of the American Meteorological Society*, **96** (9), 1545–
424 1560, doi:[10.1175/BAMS-D-13-00193.1](https://doi.org/10.1175/BAMS-D-13-00193.1), URL <http://dx.doi.org/10.1175/BAMS-D-13-00193.1>,
425 1.
- 426 Diamond, H. J., and Coauthors, 2013: US climate reference network after one decade of opera-
427 tions: Status and assessment. *Bulletin of the American Meteorological Society*, **94** (4), 485–498.

- 428 Hardin, A. W., 2015: Assessment of urban heat islands during hot weather in the u.s. northeast and
429 linkages to microscale thermal and radiational properties. M.S. thesis, Texas Tech University.
- 430 Harlan, S. L., J. H. Declet-Barreto, W. L. Stefanov, and D. B. Petitti, 2013: Neighborhood effects
431 on heat deaths: social and environmental predictors of vulnerability in maricopa county, arizona.
432 *Environmental Health Perspectives (Online)*, **121** (2), 197.
- 433 Ho, H. C., A. Knudby, P. Sirovyak, Y. Xu, M. Hodul, and S. B. Henderson, 2014: Mapping
434 maximum urban air temperature on hot summer days. *Remote Sensing of Environment*, **154**,
435 38 – 45, doi:<http://dx.doi.org/10.1016/j.rse.2014.08.012>, URL <http://www.sciencedirect.com/science/article/pii/S0034425714003095>.
- 437 Ho, H. C., A. Knudby, Y. Xu, M. Hodul, and M. Aminipour, 2016: A comparison of urban heat
438 islands mapped using skin temperature, air temperature, and apparent temperature (humidex),
439 for the greater vancouver area. *Science of the Total Environment*, **544**, 929–938.
- 440 Hondula, D. M., R. E. Davis, M. J. Leisten, M. V. Saha, L. M. Veazey, and C. R. Wegner, 2012:
441 Fine-scale spatial variability of heat-related mortality in Philadelphia County, usa, from 1983-
442 2008: a case-series analysis. *Environmental health*, **11** (1), 1.
- 443 Huang, G., W. Zhou, and M. Cadenasso, 2011: Is everyone hot in the city? spatial pat-
444 tern of land surface temperatures, land cover and neighborhood socioeconomic characteris-
445 tics in Baltimore, MD. *Journal of Environmental Management*, **92** (7), 1753 – 1759, doi:
446 <http://dx.doi.org/10.1016/j.jenvman.2011.02.006>, URL <http://www.sciencedirect.com/science/article/pii/S0301479711000454>.
- 448 IPCC, 2013: *Summary for Policymakers*. In: *Climate Change 2013: The Physical Science Basis*.
449 *Contribution of Working Group I to the Fifth Assessment Report of the Intergovernmental Panel*

450 *on Climate Change*. Cambridge University Press, Cambridge, United Kingdom and New York,
451 NY, USA.

452 Jiménez-Muñoz, J. C., and J. A. Sobrino, 2003: A generalized single-channel method for re-
453 trieving land surface temperature from remote sensing data. *Journal of Geophysical Research:*
454 *Atmospheres*, **108** (D22), n/a–n/a, doi:10.1029/2003JD003480, URL <http://dx.doi.org/10.1029/2003JD003480>.

456 Jones, E., T. Oliphant, P. Peterson, and Coauthors, 2001: SciPy: Open source scientific tools for
457 Python. URL <http://www.scipy.org/>, [Online; accessed 2016-01-01].

458 Jonsson, P., 2004: Vegetation as an urban climate control in the subtropical city of Gaborone,
459 Botswana. *International Journal of Climatology*, **24** (10), 1307–1322, doi:10.1002/joc.1064,
460 URL <http://dx.doi.org/10.1002/joc.1064>.

461 Kleerekoper, L., M. van Esch, and T. B. Salcedo, 2012: How to make a city climate-proof, ad-
462 dressing the urban heat island effect. *Resources, Conservation and Recycling*, **64**, 30–38.

463 Kloog, I., F. Nordio, B. A. Coull, and J. Schwartz, 2014: Predicting spatiotemporal mean air tem-
464 perature using {MODIS} satellite surface temperature measurements across the northeastern
465 {USA}. *Remote Sensing of Environment*, **150**, 132 – 139, doi:<http://dx.doi.org/10.1016/j.rse.2014.04.024>, URL <http://www.sciencedirect.com/science/article/pii/S0034425714001758>.

467 Laaidi, K., A. Zeghnoun, B. Dousset, P. Bretin, S. Vandentorren, E. Giraudet, and P. Beaudeau,
468 2012: The impact of heat islands on mortality in Paris during the august 2003 heat wave. *Envi-
469 ronmental health perspectives*, **120** (2), 254.

- 470 Landsberg, H. E., 1979: Atmospheric changes in a growing community (the Columbia, Mary-
471 land experience). *Urban Ecology*, **4** (1), 53 – 81, doi:[http://dx.doi.org/10.1016/0304-4009\(79\)
472 90023-8](http://dx.doi.org/10.1016/0304-4009(79)90023-8), URL <http://www.sciencedirect.com/science/article/pii/0304400979900238>.
- 473 Liang, S., 2001: Narrowband to broadband conversions of land surface albedo i: Algorithms. *Re-
474 mote Sensing of Environment*, **76** (2), 213 – 238, doi:[http://dx.doi.org/10.1016/S0034-4257\(00\)002054](http://dx.doi.org/10.1016/S0034-4257(00)
475 00205-4). URL <http://www.sciencedirect.com/science/article/pii/S0034425700002054>.
- 476 LP DAAC, 2015: Landsat8. Tech. rep., NASA Land Processes Distributed Active Archive Center
477 Products, USGS/EROS, Sioux Falls, SD.
- 478 Mikami, T., H. Ando, W. Morishima, T. Izumi, and T. Shioda, 2003: A new urban heat island
479 monitoring system in Tokyo. *Proc. Fifth Int. Conf. on Urban Climate*, International Association
480 for Urban Climate Lodz, Poland, O–3.
- 481 Nichol, J. E., W. Y. Fung, K. se Lam, and M. S. Wong, 2009: Urban heat island diagnosis using
482 ASTER satellite images and ‘in situ’ air temperature. *Atmospheric Research*, **94** (2), 276 –
483 284, doi:<http://dx.doi.org/10.1016/j.atmosres.2009.06.011>, URL <http://www.sciencedirect.com/science/article/pii/S0169809509001781>.
- 485 Nichol, J. E., and P. H. To, 2012: Temporal characteristics of thermal satellite images for ur-
486 ban heat stress and heat island mapping. *ISPRS Journal of Photogrammetry and Remote Sens-
487 ing*, **74**, 153 – 162, doi:<http://dx.doi.org/10.1016/j.isprsjprs.2012.09.007>, URL <http://www.sciencedirect.com/science/article/pii/S0924271612001761>.
- 489 Oke, T., G. Johnson, D. Steyn, and I. Watson, 1991: Simulation of surface urban heat islands under
490 ‘ideal’ conditions at night part 2: diagnosis of causation. *Boundary-Layer Meteorology*, **56** (4),
491 339–358.

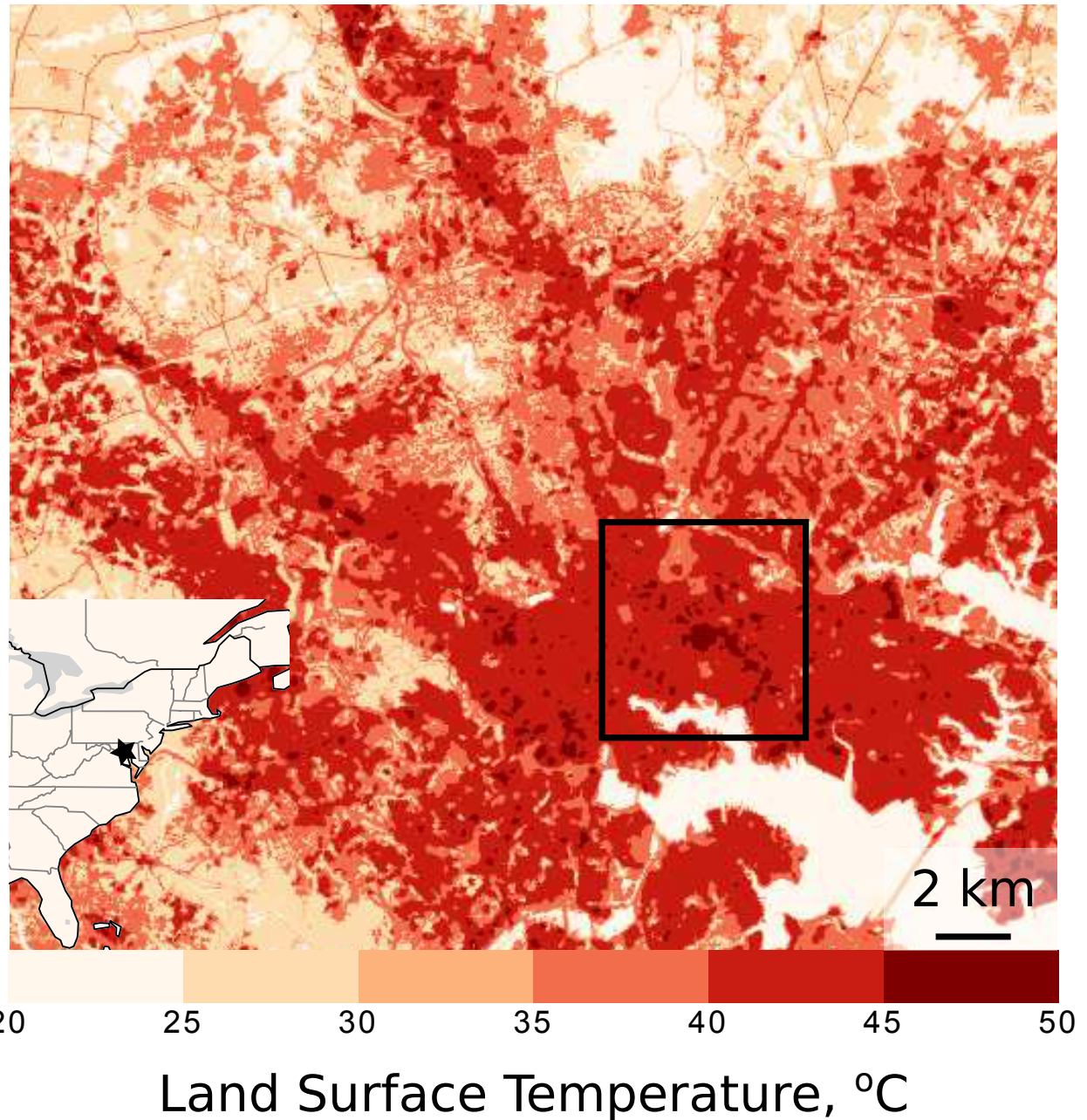
- 492 Oke, T. R., 1982: The energetic basis of the urban heat island. *Quarterly Journal of the Royal*
493 *Meteorological Society*, **108 (455)**, 1–24.
- 494 Peel, M. C., B. L. Finlayson, and T. A. Mcmahon, 2007: Updated world map of the Köppen-Geiger
495 climate classification. *Hydrology and Earth System Sciences Discussions*, **4 (2)**, 439–473, URL
496 <https://hal.archives-ouvertes.fr/hal-00298818>.
- 497 Qin, Z., A. Karnieli, and P. Berliner, 2001: A mono-window algorithm for retrieving
498 land surface temperature from landsat tm data and its application to the israel-egypt bor-
499 der region. *International Journal of Remote Sensing*, **22 (18)**, 3719–3746, doi:10.1080/
500 01431160010006971, URL <http://dx.doi.org/10.1080/01431160010006971>, <http://dx.doi.org/10.1080/01431160010006971>.
- 501
- 502 Schatz, J., and C. J. Kucharik, 2014: Seasonality of the urban heat island effect in Madison,
503 Wisconsin. *Journal of Applied Meteorology and Climatology*, **53 (10)**, 2371–2386, doi:10.1175/
504 JAMC-D-14-0107.1, URL <http://dx.doi.org/10.1175/JAMC-D-14-0107.1>, <http://dx.doi.org/10.1175/JAMC-D-14-0107.1>.
- 505
- 506 Scott, A. A., B. Zaitchik, D. Waugh, K. O'Meara, C. Hickman, and S. Stoerkel, 2016: Data
507 associated with Scott et al 2016, Intra-urban temperature variability in Baltimore. *Johns Hopkins*
508 *University Data Archive*, doi:<http://doi.org/10.7281/T10Z715B>.
- 509
- 510 Smargiassi, A., M. S. Goldberg, C. Plante, M. Fournier, Y. Baudouin, and T. Kosatsky, 2009:
511 Variation of daily warm season mortality as a function of micro-urban heat islands. *Journal of*
Epidemiology and Community Health, **63 (8)**, 659–664.
- 512
- 513 Smith, R. B., 2010: The heat budget of the earth's surface deduced from space. Tech. rep., Yale,
http://www.yale.edu/ceo/Documentation/Landsat_DN_to_Albedo.pdf.

- 514 Smoliak, B. V., P. K. Snyder, T. E. Twine, P. M. Mykleby, and W. F. Hertel, 2015: Dense network
515 observations of the Twin Cities canopy-layer urban heat island*. *Journal of Applied Meteorol-*
516 *ogy and Climatology*, **54** (9), 1899–1917.
- 517 Stewart, I. D., and T. R. Oke, 2012: Local climate zones for urban temperature stud-
518 ies. *Bulletin of the American Meteorological Society*, **93** (12), 1879–1900, doi:10.1175/
519 BAMS-D-11-00019.1, URL <http://dx.doi.org/10.1175/BAMS-D-11-00019.1>, <http://dx.doi.org/10.1175/BAMS-D-11-00019.1>.
- 520
- 521 Sun, Y.-J., J.-F. Wang, R.-H. Zhang, R. Gillies, Y. Xue, and Y.-C. Bo, 2005: Air temperature
522 retrieval from remote sensing data based on thermodynamics. *Theoretical and applied climatol-*
523 *ogy*, **80** (1), 37–48.
- 524
- 525 USGS, 2015: MD/PA sandy supplemental lidar data acquisition and processing production task
USGS contract no. g10pc00057. Tech. rep., United States Geological Survey.
- 526
- 527 Voogt, J., and T. Oke, 2003: Thermal remote sensing of urban climates. *Remote Sensing of*
528 *Environment*, **86** (3), 370 – 384, doi:[http://dx.doi.org/10.1016/S0034-4257\(03\)00079-8](http://dx.doi.org/10.1016/S0034-4257(03)00079-8), URL
<http://www.sciencedirect.com/science/article/pii/S0034425703000798>, urban Remote Sensing.
- 529
- 530 White-Newsome, J. L., S. J. Brines, D. G. Brown, J. T. Dvonch, C. J. Gronlund, K. Zhang, E. M.
531 Oswald, and M. S. O'Neill, 2013: Validating satellite-derived land surface temperature with in
532 situ measurements: a public health perspective. *Environmental Health Perspectives (Online)*,
121 (8), 925.
- 533
- 534 WMO, 2010: WMO guide to meteorological instruments and methods of observation. Tech. Rep.
No. 8, World Meteorological Organization.

- 535 WMO, 2014: *Atlas of mortality and economic losses from weather, climate, and water extremes*
536 (1970-2012). Geneva, Switzerland : World Meteorological Organization, URL <https://search.library.wisc.edu/catalog/9910206226102121>.
- 537
- 538 Xu, Y., and Y. Liu, 2015: Monitoring the near-surface urban heat island in beijing, china by
539 satellite remote sensing. *Geographical Research*, **53** (1), 16–25.
- 540 Zaitchik, B. F., K. O'Meara, K. Baja, A. A. Scott, D. W. Waugh, and M. C. McCormack, 2016:
541 B'more Cool: Monitoring the urban heat island at high density for health and urban design.
- 542 Zhao, L., X. Lee, R. B. Smith, and K. Oleson, 2014: Strong contributions of local background
543 climate to urban heat islands. *Nature*, **511** (7508), 216–219, URL <http://dx.doi.org/10.1038/nature13462>.
- 544

545 LIST OF FIGURES

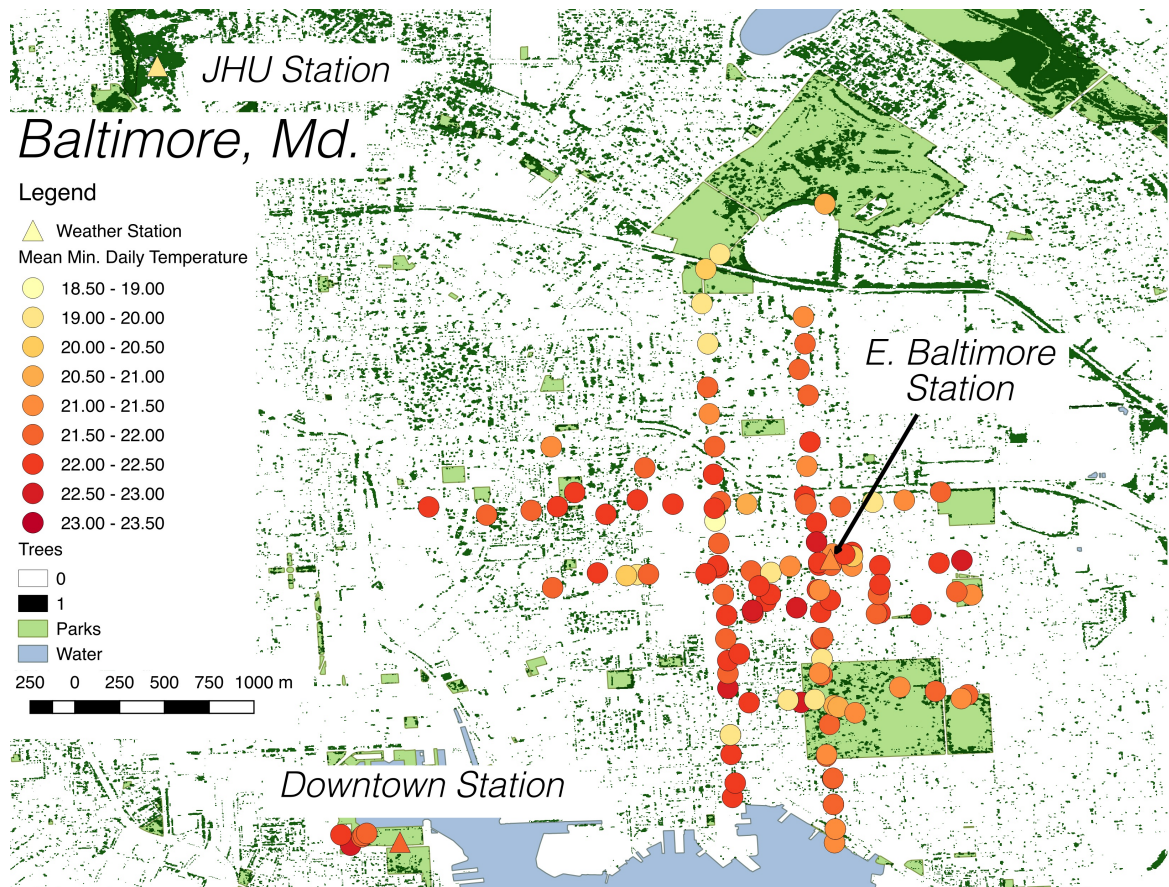
546	Fig. 1. A thermal land-surface temperature map of Baltimore, Maryland, USA from Landsat 8 (LP 547 DAAC 2015) on July 2015. The boxed inset surrounds the neighborhoods of focus in this 548 study.	27
549	Fig. 2. Two examples of sensors deployed in trees in an underserved East Baltimore neighborhood 550 characterized by low tree cover, large percent impervious surfaces as well as high vacancy 551 rates. Site a) typifies a park or green space and was listed as green space and partial shade 552 while b) is characteristic of an impervious streetscape and listed as impervious and partial 553 shade.	28
554	Fig. 3. Locations of the 135 sensors in East Baltimore. Color shows \bar{T} , the temporal mean of daily 555 minimum temperatures for June 1-September 15, 2015.	29
556	Fig. 4. A summary of the difference between selected iButtons and weather stations located a) 557 at JHU and b) downtown. Each column represents the distribution of 68 measurements 558 from one iButton sensor minus the station for daily minimum temperature for July 10- 559 September 15, 2015. Red lines represent the median of the data, the blue box represents 560 the interquartile range ($IQR = [Q1, Q3]$), and black lines represent the wide interquartile 561 range, $[Q1 - 1.5 \cdot IQR, Q3 + 1.5 \cdot IQR]$. Outliers outside of this range are shown as +; for 562 the JHU station evaluation, one outlier from each column ranging from $5 - 6^{\circ}\text{C}$ is omitted. 563 The shaded area is the accuracy of the iButton, $\pm 0.5^{\circ}\text{C}$	30
564	Fig. 5. Histogram (a,c) and time series (b,d) of the E. Baltimore temperature data (a,b) and the 565 difference with the downtown station (c,d) for daily minimum temperature for sensors. The 566 station data count in a) is inflated by a factor of 100 to appear on the same scale as the iButton 567 data. Green and orange lines represent sensors located in green spaces and impervious 568 spaces, respectively. An extreme temperature threshold (b, light gray) represents the 95 th 569 percentile of temperature for the period 2000-2015. Difference with the downtown station 570 in (c) is calculated as $\Delta T = T_i - T_{\text{downtown}}$, and spatially averaged in d) to compute $\langle \Delta T(t) \rangle =$ 571 $\langle T_i - T_{\text{downtown}} \rangle$ for $i \in \{\text{impervious, green space}\}$. Error bars in d) give the spatial standard 572 deviation, representing sensor to sensor variability.	31
573	Fig. 6. The relationship between meteorology and the downtown station. Left: relationship between 574 meteorological variables and temperature differences $\bar{\Delta T} = \langle T_{\text{sensor}} - T_{\text{downtown}} \rangle$. Right: re- 575 lationship between meteorological variables and spatial variability within E. Baltimore as 576 shown by $\sigma_{\Delta T} = \sigma(T_{\text{sensor}} - T_{\text{downtown}})$, the spatial standard deviation of agreement with 577 the downtown station. Meteorological variables come from the JHU station; shown are 578 daily averages lagged by one day. The correlation coefficient r is calculated as the Pearson 579 product-moment correlation coefficient.	32
580	Fig. 7. Relationship between \bar{T} and surface properties at each sensor located in green spaces (left) 581 and impervious spaces (right) as well as the Pearson product-moment correlation coefficient 582 r	33
583	Fig. 8. Relationship between \bar{T} and LST (Landsat 8) at each sensor located in green spaces (left) 584 and impervious spaces (right) as well as the Pearson product-moment correlation coefficient 585 r	34



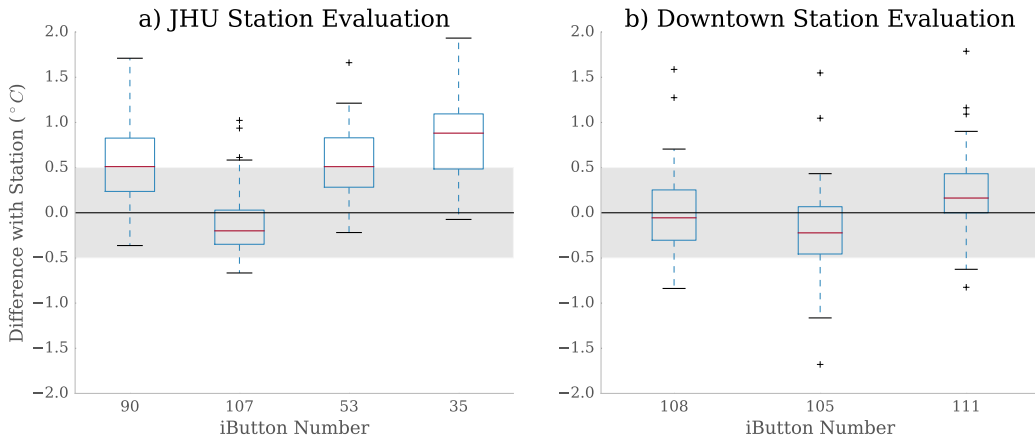
586 FIG. 1. A thermal land-surface temperature map of Baltimore, Maryland, USA from Landsat 8 (LP DAAC
587 2015) on July 2015. The boxed inset surrounds the neighborhoods of focus in this study.



588 FIG. 2. Two examples of sensors deployed in trees in an underserved East Baltimore neighborhood charac-
589 terized by low tree cover, large percent impervious surfaces as well as high vacancy rates. Site a) typifies a
590 park or green space and was listed as green space and partial shade while b) is characteristic of an impervious
591 streetscape and listed as impervious and partial shade.



592 FIG. 3. Locations of the 135 sensors in East Baltimore. Color shows \bar{T} , the temporal mean of daily minimum
593 temperatures for June 1-September 15, 2015.



594 FIG. 4. A summary of the difference between selected iButtons and weather stations located a) at JHU and
 595 b) downtown. Each column represents the distribution of 68 measurements from one iButton sensor minus
 596 the station for daily minimum temperature for July 10-September 15, 2015. Red lines represent the median of
 597 the data, the blue box represents the interquartile range ($IQR = [Q_1, Q_3]$), and black lines represent the wide
 598 interquartile range, $[Q_1 - 1.5 \cdot IQR, Q_3 + 1.5 \cdot IQR]$. Outliers outside of this range are shown as +; for the JHU
 599 station evaluation, one outlier from each column ranging from $5 - 6^{\circ}\text{C}$ is omitted. The shaded area is the
 600 accuracy of the iButton, $\pm 0.5^{\circ}\text{C}$.

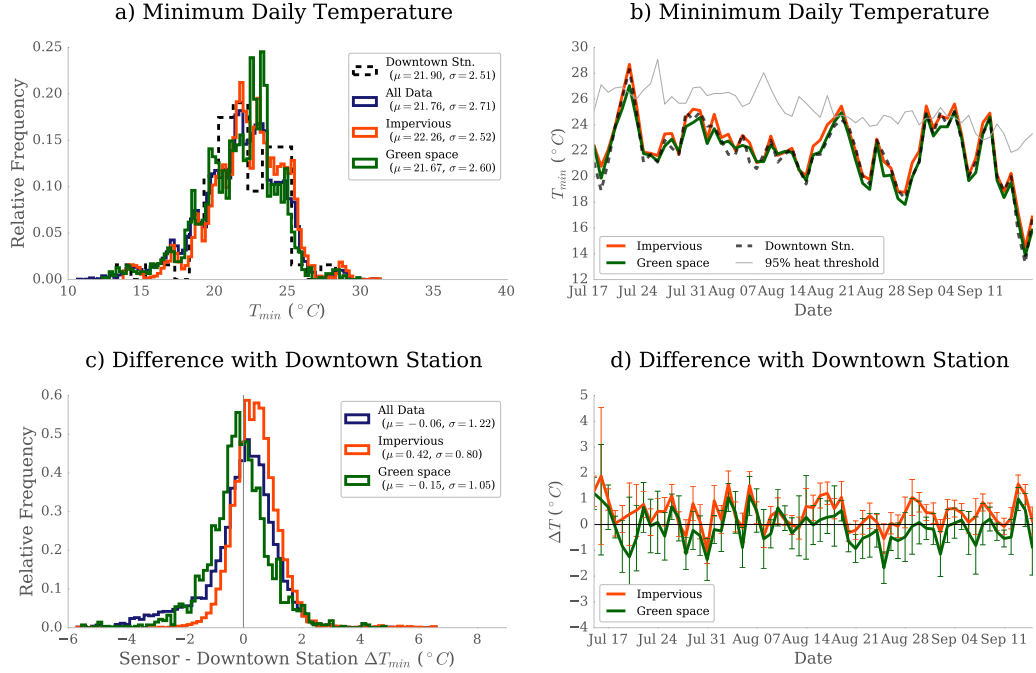
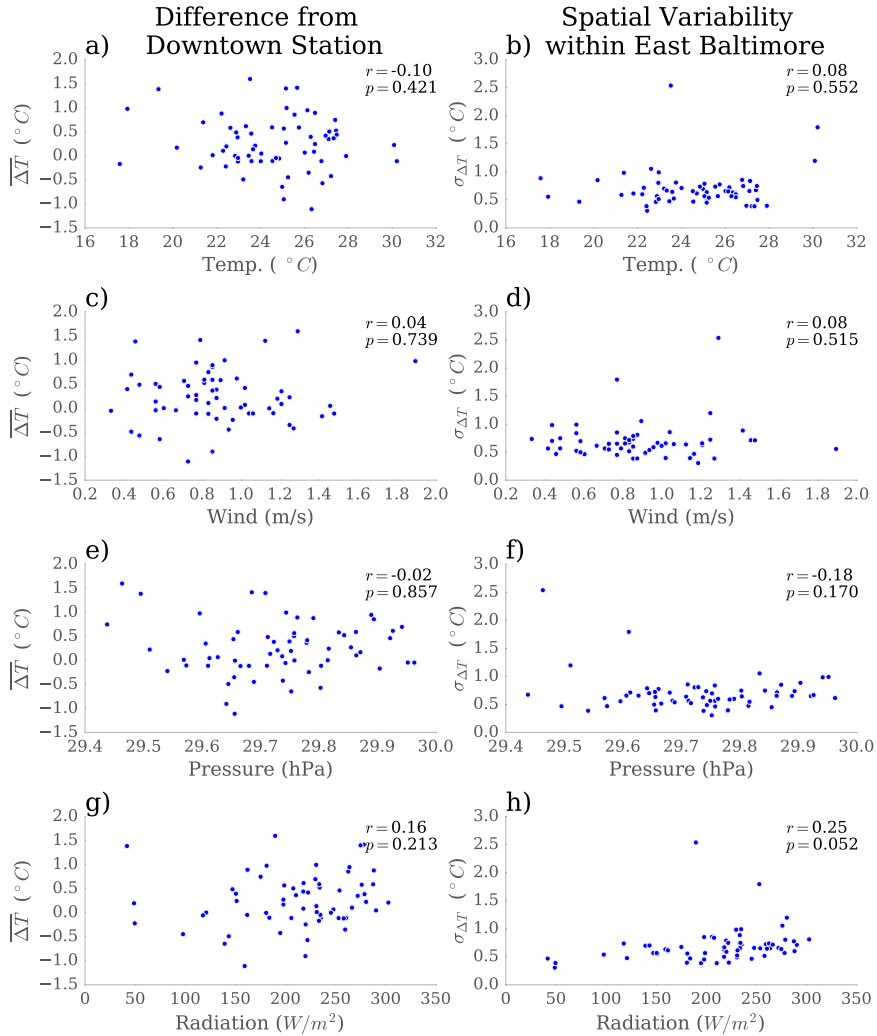
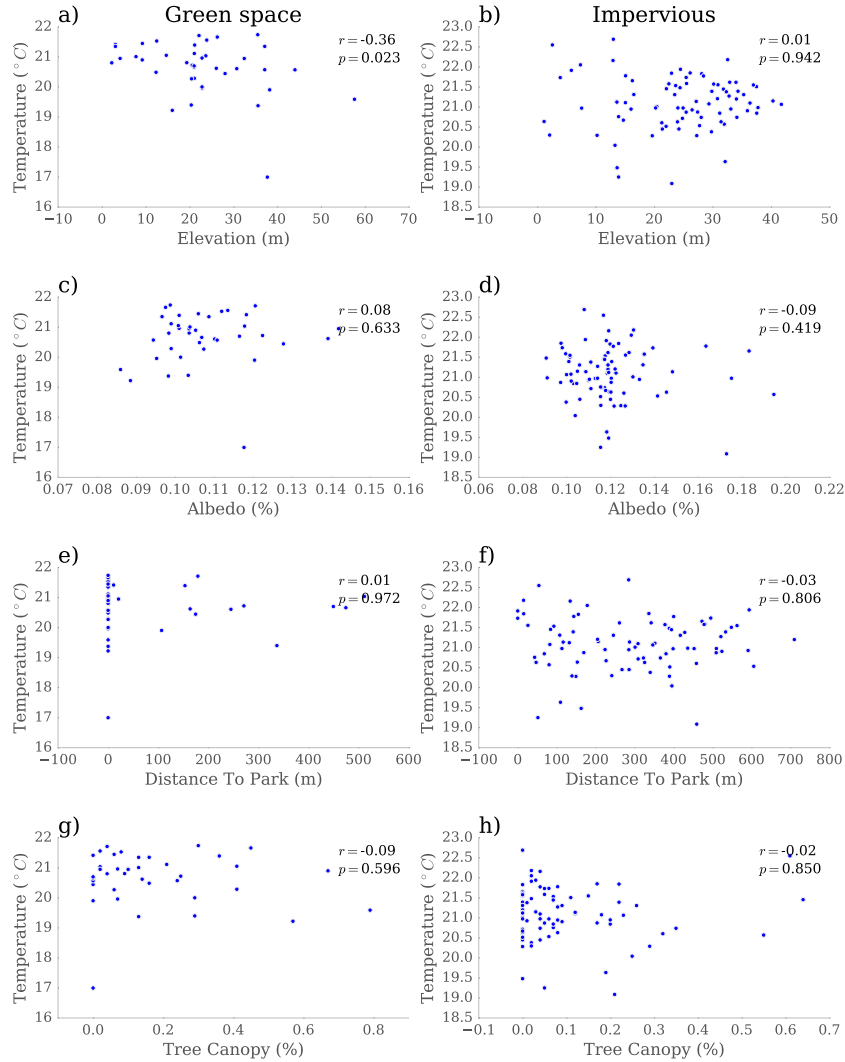


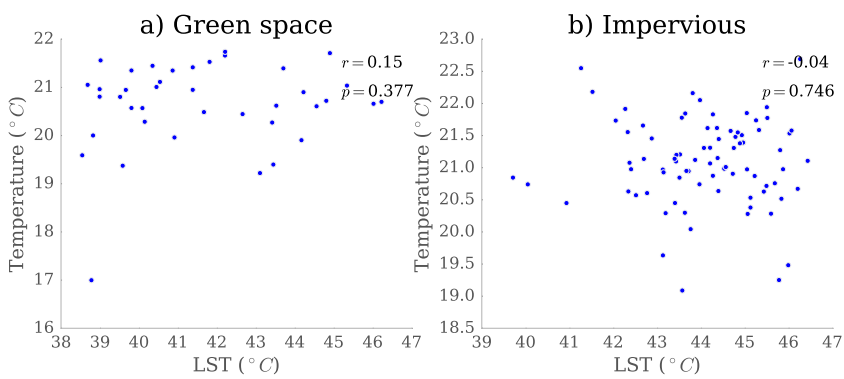
FIG. 5. Histogram (a,c) and time series (b,d) of the E. Baltimore temperature data (a,b) and the difference with the downtown station (c,d) for daily minimum temperature for sensors. The station data count in a) is inflated by a factor of 100 to appear on the same scale as the iButton data. Green and orange lines represent sensors located in green spaces and impervious spaces, respectively. An extreme temperature threshold (b, light gray) represents the 95th percentile of temperature for the period 2000-2015. Difference with the downtown station in (c) is calculated as $\Delta T = T_i - T_{downtown}$, and spatially averaged in d) to compute $\langle \Delta T(t) \rangle = \langle T_i - T_{downtown} \rangle$ for $i \in \{\text{impervious, green space}\}$. Error bars in d) give the spatial standard deviation, representing sensor to sensor variability.



609 FIG. 6. The relationship between meteorology and the downtown station. Left: relationship between mete-
 610 orological variables and temperature differences $\bar{\Delta}T = \langle T_{\text{sensor}} - T_{\text{downtown}} \rangle$. Right: relationship between mete-
 611 orological variables and spatial variability within E. Baltimore as shown by $\sigma_{\Delta T} = \sigma(T_{\text{sensor}} - T_{\text{downtown}})$, the
 612 spatial standard deviation of agreement with the downtown station. Meteorological variables come from the JHU
 613 station; shown are daily averages lagged by one day. The correlation coefficient r is calculated as the Pearson
 614 product-moment correlation coefficient.



615 FIG. 7. Relationship between \bar{T} and surface properties at each sensor located in green spaces (left) and
 616 impervious spaces (right) as well as the Pearson product-moment correlation coefficient r .



617 FIG. 8. Relationship between \bar{T} and LST (Landsat 8) at each sensor located in green spaces (left) and imper-
618 vious spaces (right) as well as the Pearson product-moment correlation coefficient r .